3rd Specialty Conference on Material Engineering & Applied Mechanics
3e Conférence spécialisée sur le génie des matériaux et mécanique appliquée

Montréal, Québec
May 29 to June 1, 2013 / *29 mai au 1 juin 2013*

Harmonic Response of Doubly symmetric Thin-walled Members based on the Vlasov Theory – II. Finite Element Formulation

Mohammed Ali Hjaji[1] and Magdi Mohareb[2]

[1] Department of Mechanical and Industrial Engineering, Tripoli University, Tripoli, Libya
[2] Department of civil engineering, University of Ottawa, Ottawa, Canada

Abstract: A finite element formulation is developed for the steady state analysis of doubly symmetric thin-walled members subjected to harmonic forces. The formulation is based on the Vlasov beam assumptions. A family of exact shape functions is formulated based on the closed form solutions of the governing equations. The shape functions are then used to formulate the mass and stiffness matrices and the energy equivalent load vector. The finite element is applicable to prismatic thin-walled of doubly symmetric open cross-sections and captures the St. Venant and warping deformation effects, as well as translational and rotary inertia. Comparisons are provided against other established solutions to assess the accuracy and efficiency of the finite element. The results based on the present finite element formulation are observed to be free from the discretization errors. As a result, accurate solutions are obtained while keeping the number of degrees of freedom to a minimum.

1. Literature Review on Finite Element Formulations and Scope

The literature focuses on finite element formulations for the dynamic analysis of open thin-walled members. In general, finite element are based on three approaches of shape functions; (1) approximate polynomial interpolation functions, (2) shape functions based on the exact solution of the static equilibrium equations, and (3) shape functions based on exact solution of the dynamic equations of motion. Most finite element formulations developed are based on the approximate shape functions including the work of Chen and Tamma (1994), Lee and Kim (2002a, b), Kim and Kim (2005), Voros (2008, 2009), Vo and Lee (2009, 2010) and Vo et al. (2010, 2011). Among them, Chen and Tamma (1994) used the finite element method in conjunction with an implicit-starting unconditionally stable methodology for the dynamic analysis of thin-walled open members under deterministic loads. Hashemi and Richard (2000a) studied the coupled bending–torsional vibration analysis of thin-walled beams by developing a dynamic finite element. Their solution can be regarded as an intermediate method between the finite element method and the dynamic stiffness matrix method. The exact solutions of the governing dynamic equations of equilibrium were obtained and, subsequently, frequency-dependent hyperbolic interpolation functions were adopted to formulate the stiffness and mass matrices of the structure. Later on, Hashemi and Richard (2000b) extended their work to include the effect of axial force. By using linear and cubic Hermitian shape functions, Lee and Kim (2002a, 2002b) investigated the coupled free vibration of thin-walled composite beams with doubly symmetric and channel-shaped cross-sections. Kim and Kim (2005) derived the coupled bending-torsional free vibration of asymmetric thin-walled shear deformable beam by using an isoparametric finite beam element. The influence of lateral forces on the coupled bending-torsional free vibration of thin-walled open members was studied by Voros (2008, 2009). In his formulations, a two-noded beam element with fourteen degrees of freedom is formulated. Recently, Vo and Lee (2009, 2010) and Vo et al. (2010, 2011) studied the coupled flexural-torsional free vibration of thin-walled open composite beams under constant axial forces and end moments by developing a displacement-based one dimensional finite element model. Formulations based on the exact solution for

static equilibrium equations include the work of Mei (1970) and Hu et al. (1996). They have the advantage of avoiding locking problems which could arise in some of the solutions based on polynomial interpolation. Finite element solutions based on exact homogeneous solution of the dynamic equations of motion include the work of Hjaji and Mohareb (2011) and offer two advantages: (1) it eliminates the discretization errors encountered in other finite element formulations, and thus it converges to the solution using a minimum number of degrees of freedom, and (2) it lead to elements that are free from shear locking arising from the approximate interpolation functions.

This paper aims at developing a finite element formulation for dynamic analysis of doubly symmetric thin-walled open members subjected to harmonic forces, in which the St. Venant and warping torsional effects, the translational and rotary inertias effects are incorporated. The present paper develops an efficient finite element based on exact shape functions that exactly satisfy the homogeneous form of the governing field equations of motion. The exact shape functions developed in the companion paper (Hjaji and Mohareb 2013) are implemented to formulate the exact stiffness, mass matrices and the associated load potential vector in finite element formulation.

2. Main Assumptions

The formulation is based on the following assumptions:

1. Cross-sections are assumed open and doubly symmetric,
2. Cross-sections are assumed to remain undeformed in their own plane but free to undergo warping deformation in the longitudinal direction,
3. Transverse shear deformation are neglected,
4. Material is assumed linearly elastic, and
5. The strains and rotations are assumed small.

3. Displacement Fields

Based on the above assumptions, the longitudinal displacement $w_p(z,s,t)$ and the mid-surface ad displacement components $u_p(z,s,t)$ and $v_p(z,s,t)$ at a general point $p(x,y)$ located on the mid-surface of the cross-section (Fig. 1a) can be expressed in terms of displacements $\bar{u}(z,t)$ and $\bar{v}(z,t)$ of the shear centre S_c in the principal X and Y directions and the rotation angle $\theta_z(z,t)$ about longitudinal axis [Vlasov 1961] as:

[1] $$w_p(z,s,t) = w(z,t) - x(s)u'(z,t) - y(s)v'(z,t) - \omega(s)\theta_z'(z,t)$$

[2-3] $$u_p(z,s,t) = u(z,t) - y(s)\theta_z(z,t), \text{ and } v_p(z,s,t) = v(z,t) + x(s)\theta_z(z,t)$$

in which $w(z,t)$ is the average longitudinal displacement along Z axis, $x(s)$ and $y(s)$ are the coordinates of point p along the principal axes, and $\omega(s)$ is the warping function defined by $\omega(s) = \int_A h(s)dA$ [Vlasov 1961]. In the present formulation, since the applied longitudinal loads are assumed to vanish, and since the longitudinal equation of motion is uncoupled from the other equations of motion [Hjaji and Mohareb 2013a], the average longitudinal displacement $w(z,t)$ will equally vanish. All primes denote derivatives with respect to space coordinate z .

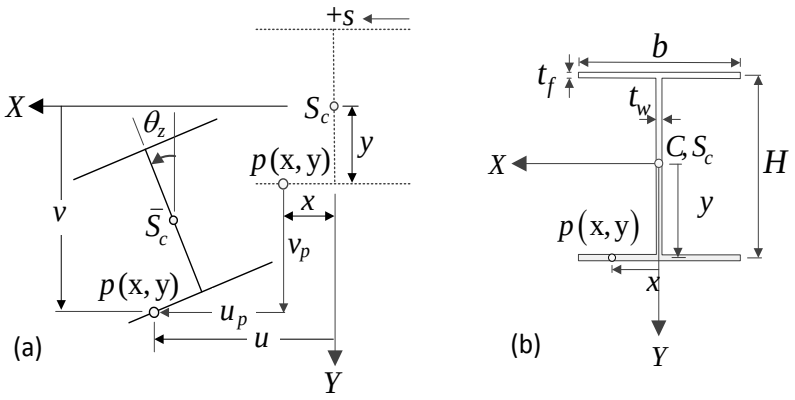

Figure (1): Coordinate system and displacement fields

4. Expressions for Force Functions

The applied harmonic forces are assumed to have an exciting frequency Ω and are given by:

[4] $$q_x(z,t), q_y(z,t), m_z(z,t) = \left[\bar{q}_x(z), \bar{q}_y(z), \bar{m}_z(z)\right] e^{i\Omega t}$$, and

[5] $$V_x(z_e,t), V_y(z_e,t), M_z(z_e,t), M_x(z_e,t), M_y(z_e,t), M_w(z_e,t) = \left[\bar{V}_x(z_e), \bar{V}_y(z_e), \bar{M}_z(z_e), \bar{M}_x(z_e), \bar{M}_y(z_e), \bar{M}_w(z_e)\right] e^{i\Omega t}$$

where $i = \sqrt{-1}$ is the imaginary constant, $q_j(z,t)$ for $j = x, y$, are the distributed lateral and transverse forces, $m_z(z,t)$ is the distributed twisting moment, $V_x(z_e,t)$ and $V_y(z_e,t)$ are the concentrated lateral and transverse forces, $M_j(z_e,t)$ for $j = x, y, z$ are the end moments and $M_j(z_e,t)$ is the end bimoments, all harmonic forces and moments applied at beam ends (i.e., $z_e = 0, \ell$) and assumed to have the same sign convention as those of the end displacements (Fig. 1).

5. Expressions for Displacement Fields

Under the above applied harmonic forces, the steady state displacements at the mid-surface are harmonic, i.e.,

[6] $$u(z,t), v(z,t), \theta_z(z,t) = \left[\bar{u}(z), \bar{v}(z), \bar{\theta}_z(z)\right] e^{i\Omega t}$$

where $\bar{u}(z), \bar{v}(z)$ and $\bar{\theta}_z(z)$ are space functions for lateral, transverse, and torsional responses, respectively. In line with the objective of this study, the displacement functions in Equation (6) neglect the transient response.

6. Hamilton's Variational Formulation

The variational form of Hamiltonian functional is taken to be stationary, i.e.,

[7] $$\int_{t_1}^{t_2}\delta\left(T^{*}-U^{*}\right)dt+\int_{t_1}^{t_2}\delta W^{*}dt=0$$

in which δT is the variation of the kinetic energy, δU is the variation of the internal strain energy, δW is the variation of the work done due to applied forces, while the integration is performed between arbitrary time limits t_1 and t_2. The expressions for energy variations are given as [e.g. Librescu 2006]:

[8-9] $$\delta T^{*}=\int_A \rho\left[\dot{u}_p\delta\dot{u}_p+\dot{v}_p\delta\dot{v}_p+\dot{w}_p\delta\dot{w}_p\right]dz\ ,\ \delta U^{*}=\int_0^{\ell}\int_A E\,\varepsilon_{zz}\,\delta\varepsilon_{zz}\,dA\,dz+\int_0^{\ell}GJ\,\theta_z'\,\delta\theta_z'dz$$, and

[10]
$$\begin{aligned}\delta W^{*}=&\left[V_x\left(z_e,t\right)\delta u\left(z_e,t\right)\right]_0^{\ell}+\left[V_y\left(z_e,t\right)\delta w\left(z_e,t\right)\right]_0^{\ell}+\left[M_x\left(z_e,t\right)\delta v'\left(z_e,t\right)\right]_0^{\ell}\\&+\left[M_y\left(z_e,t\right)\delta u'\left(z_e,t\right)\right]_0^{\ell}+\left[M_z\left(z_e,t\right)\delta\theta_z\left(z_e,t\right)\right]_0^{\ell}+\left[M_w\left(z_e,t\right)\delta\theta_z'\left(z_e,t\right)\right]_0^{\ell}\\&+\int_0^{\ell}\left[q_z\left(z,t\right)\delta w\left(z,t\right)+q_x\left(z,t\right)\delta u\left(z,t\right)+q_y\left(z,t\right)\delta v\left(z,t\right)+m_z\left(z,t\right)\delta\theta_z\left(z,t\right)\right]dz\end{aligned}$$

in which $\varepsilon_{zz}\approx\partial w_p/\partial z$ is the longitudinal strain, E is the modulus of elasticity, G is the shear modulus, ρ is the material density, J is the St. Venant torsion constant and A is the area of the cross-section, and all dots denote the derivatives with respect to time t.

From Equations (1-6), by substituting into energy term expressions (8-10), and the resulting expressions into Hamilton's principle (Eq. 7), performing integration by parts and enforcing the orthogonality conditions $\int_A\left[x\left(s\right),y\left(s\right),x\left(s\right)y\left(s\right),x\left(s\right)\omega(s),y\left(s\right)\omega(s),\omega(s)\right]dA=0$, yields:

[11]
$$\begin{aligned}\int_0^{\ell}\Big[&EI_{yy}\bar{u}''\delta\bar{u}''+EI_{xx}\bar{v}''\delta\bar{v}''+EC_w\,\bar{\theta}_z''\delta\bar{\theta}_z''+GJ\,\bar{\theta}_z'\delta\bar{\theta}_z'-\bar{q}_x\left(z\right)\delta\bar{u}-\bar{q}_y\left(z\right)\delta\bar{v}-\bar{m}_z\left(z\right)\delta\bar{\theta}_z\\&-\Omega^2\left(\rho A\,\bar{u}\,\delta\bar{u}+\rho A\,\bar{v}\,\delta\bar{v}+\rho A r_o^2\,\bar{\theta}_z\,\delta\bar{\theta}_z+\rho I_{yy}\,\bar{u}'\delta\bar{u}'+\rho I_{xx}\,\bar{v}'\delta\bar{v}'+\rho C_w\,\bar{\theta}_z'\,\delta\bar{\theta}_z'\right)\Big]dz\\&-\Big[\bar{V}_x\left(z_e\right)\delta\bar{u}\left(z_e\right)+\bar{V}_y\left(z_e\right)\delta\bar{v}\left(z_e\right)+\bar{M}_x\left(z_e\right)\delta\bar{v}'\left(z_e\right)+\bar{M}_y\left(z_e\right)\delta\bar{u}'\left(z_e\right)\\&+\bar{M}_z\left(z_e\right)\delta\bar{\theta}_z\left(z_e\right)+\bar{M}_w\left(z_e\right)\delta\bar{\theta}_z'\left(z_e\right)\Big]_0^{\ell}=0\end{aligned}$$

In which $r_o^2=\left(I_{xx}+I_{yy}\right)/A$.

7. Formulating Exact Shape Functions

The homogeneous solutions of the governing equilibrium equations related to lateral, transverse and torsional responses as derived in the companion paper (Hjaji and Mohareb 2013a) can be rewritten as:

[12-14] $$\bar{u}(z)=\left\langle E_\alpha(z)\right\rangle_{1\times4}^{T}\{A\}_{4\times1},\ \bar{v}(z)=\left\langle E_\beta(z)\right\rangle_{1\times4}^{T}\{B\}_{4\times1},\ \bar{\theta}_z(z)=\left\langle E_\gamma(z)\right\rangle_{1\times4}^{T}\{C\}_{4\times1}$$

where the vector of integration constants $\langle A\rangle_{1\times4}^T=\langle A_1\ A_2\ A_3\ A_4\rangle_{1\times14}^T$, $\langle B\rangle_{1\times4}^T=\langle B_1\ B_2\ B_3\ B_4\rangle_{1\times14}^T$, $\langle C\rangle_{1\times4}^T=\langle C_1\ C_2\ C_3\ C_4\rangle_{1\times14}^T$ and $E_\alpha(z)=\left\langle e^{\alpha_1 z}\ e^{\alpha_2 z}\ e^{\alpha_3 z}\ e^{\alpha_4 z}\right\rangle_{1\times4}^T$, $E_\beta(z)=\left\langle e^{\beta_1 z}\ e^{\beta_2 z}\ e^{\beta_3 z}\ e^{\beta_4 z}\right\rangle_{1\times4}^T$, $E_\gamma(z)=\left\langle e^{\gamma_1 z}\ e^{\gamma_2 z}\ e^{\gamma_3 z}\ e^{\gamma_4 z}\right\rangle_{1\times4}^T$, in which the roots $\beta_{1,2}=\pm\left[-q_1+(q_2)^{1/2}\right]^{1/2}$, $\beta_{3,4}=\pm i\left[q_1+(q_2)^{1/2}\right]^{1/2}$ where $q_1=\rho\Omega^2/2E$, $q_2=q_1^2-\left(\rho A/EI_{yy}\right)$. The roots α_i are obtained through similar expression after replacing I_{yy} by I_{xx}, and the roots γ_i are obtained by $\gamma_{1,2}=\pm\left[-s_1+(s_2)^{1/2}\right]^{1/2}$, $\gamma_{3,4}=\pm i\left[s_1+(s_2)^{1/2}\right]^{1/2}$, where $s_1=\left(\rho\Omega^2C_w-GJ\right)/2EC_w$ and $s_2=\rho A\Omega^2r_o^2/EC_w$.

To relate the displacement functions to the nodal displacements, the vector of integration constants $\{A\}_{4\times1}$ is expressed in terms of the nodal lateral displacements and slopes $\langle u_n\rangle_{1\times4}^T=\langle u_1\ u_2\ u_3\ u_4\rangle_{1\times4}^T$ by enforcing the conditions $\bar{u}(0)=u_1$, $\bar{u}'(0)=u_2$, $\bar{u}(\ell)=u_3$ and $\bar{u}'(\ell)=u_4$, yielding

[15] $$\{u_n\}_{4\times1}=\begin{Bmatrix}\bar{u}(0)\\ \bar{u}'(0)\\ \bar{u}(\ell)\\ \bar{u}'(\ell)\end{Bmatrix}=\begin{bmatrix}\langle E_\alpha(0)\rangle_{1\times4}^T\\ \langle E_\alpha'(0)\rangle_{1\times4}^T\\ \langle E_\alpha(\ell)\rangle_{1\times4}^T\\ \langle E_\alpha'(\ell)\rangle_{1\times4}^T\end{bmatrix}\{A\}_{4\times1}=[G_\alpha]_{4\times4}\{A\}_{4\times1}$$

From equation (15), by substituting into equation (12), one obtains:

[16] $$\bar{u}(z)=\langle E_\alpha(z)\rangle_{1\times4}^T[G_\alpha]_{4\times4}^{-1}\{u_n\}_{4\times1}=\langle H_\alpha(z)\rangle_{1\times4}^T\{u_n\}_{4\times1}$$

in which $\langle H_\alpha(z)\rangle_{1\times4}^T=\langle E_\alpha(z)\rangle_{1\times4}^T[G_\alpha]_{4\times4}^{-1}$ is the matrix of shape functions for the lateral response. It is noted that the interpolation shape functions presented in Equation (16) exactly satisfy the homogeneous form of the lateral equation (12). In a similar way, the transverse displacement $\bar{v}(z)$ and torsional rotation $\bar{\theta}_z(z)$ are expressed in terms of nodal transverse displacement $\{v_n\}_{4\times1}$ and torsional angle $\{\theta_{zn}\}_{4\times1}$ as

[17-18] $$\bar{v}(z)=\langle H_\beta(z)\rangle_{1\times4}^T\{v_n\}_{4\times1}\ \text{and}\ \bar{\theta}_z(z)=\langle H_\gamma(z)\rangle_{1\times4}^T\{\theta_{zn}\}_{4\times1}$$

where $\langle H_\beta(z)\rangle_{1\times4}^T$ and $\langle H_\gamma(z)\rangle_{1\times4}^T$ are the matrices of exact shape functions for transverse and torsional responses, given by $\langle H_\beta(z)\rangle_{1\times4}^T=\langle E_\beta(z)\rangle_{1\times4}^T[G_\beta]_{4\times4}^{-1}$, and $\langle H_\gamma(z)\rangle_{1\times4}^T=\langle E_\gamma(z)\rangle_{1\times4}^T[G_\gamma]_{4\times4}^{-1}$.

8. Finite Element Formulation

From equations (16-18), by substituting into equation (11), yielding

$$\left(\left[\begin{array}{c|c|c} [K_\alpha]_{4\times4} & [0]_{4\times4} & [0]_{4\times4} \\ \hline [0]_{4\times4} & [K_\beta]_{4\times4} & [0]_{4\times4} \\ \hline [0]_{4\times4} & [0]_{4\times4} & [K_\gamma]_{4\times4} \end{array}\right] - \Omega^2 \left[\begin{array}{c|c|c} [M_\alpha]_{4\times4} & [0]_{4\times4} & [0]_{4\times4} \\ \hline [0]_{4\times4} & [M_\beta]_{4\times4} & [0]_{4\times4} \\ \hline [0]_{4\times4} & [0]_{4\times4} & [M_\gamma]_{4\times4} \end{array}\right]\right)_{12\times12} \left\{\begin{array}{c} \{u_n\}_{4\times1} \\ \hline \{v_n\}_{4\times1} \\ \hline \{\theta_{zn}\}_{4\times1} \end{array}\right\}_{12\times1} = \left\{\begin{array}{c} \{F_{xn}\}_{4\times1} \\ \hline \{F_{yn}\}_{4\times1} \\ \hline \{F_{zn}\}_{4\times1} \end{array}\right\}_{12\times1} \tag{19}$$

in which $[K_\alpha]_{4\times4} = \int_0^\ell EI_{yy} \{H''_\alpha(z)\}_{4\times1} \langle H''_\alpha(z)\rangle_{1\times4}^T dz$, $[K_\beta]_{4\times4} = \int_0^\ell EI_{xx} \{H''_\beta(z)\}_{4\times1} \langle H''_\beta(z)\rangle_{1\times4}^T dz$, $[K_\gamma]_{4\times4} = \int_0^\ell \left[EC_w \{H''_\gamma(z)\}_{4\times1} \langle H''_\gamma(z)\rangle_{1\times4}^T + GJ \{H'_\gamma(z)\}_{4\times1} \langle H'_\gamma(z)\rangle_{1\times4}^T\right] dz$ are the element stiffness matrices for lateral, transverse and torsional responses, respectively. The element mass matrices for lateral, transverse and torsional responses are;

$[M_\alpha]_{4\times4} = \int_0^\ell \left[\rho A \{H_\alpha(z)\}_{4\times1} \langle H_\alpha(z)\rangle_{1\times4}^T + \rho I_{yy} \{H'_\alpha(z)\}_{4\times1} \langle H'_\alpha(z)\rangle_{1\times4}^T\right] dz$,

$[M_\beta]_{4\times4} = \int_0^\ell \left[\rho A \{H_\beta(z)\}_{4\times1} \langle H_\beta(z)\rangle_{1\times4}^T + \rho I_{xx} \{H'_\beta(z)\}_{4\times1} \langle H'_\beta(z)\rangle_{1\times4}^T\right] dz$, and

$[M_\gamma]_{4\times4} = \int_0^\ell \left[\rho A r_o^2 \{H_\gamma(z)\}_{4\times1} \langle H_\gamma(z)\rangle_{1\times4}^T + \rho C_w \{H'_\gamma(z)\}_{4\times1} \langle H'_\gamma(z)\rangle_{1\times4}^T\right] dz$, and the element vectors of applied lateral, transverse and torsional forces are, respectively, given by

$\{F_{xn}(z)\}_{4\times1} = \int_0^\ell \bar{q}_x \{H_\alpha(z)\}_{4\times1} dz + \left[\bar{V}_x(z) \{H_\alpha(z)\}_{4\times1}\right]_0^\ell + \left[\bar{M}_y(z) \{H'_\alpha(z)\}_{4\times1}\right]_0^\ell$,

$\{F_{yn}(z)\}_{4\times1} = \int_0^\ell \bar{q}_y \{H_\beta(z)\}_{4\times1} dz + \left[\bar{V}_y(z) \{H_\beta(z)\}_{4\times1}\right]_0^\ell + \left[\bar{M}_x(z) \{H'_\beta(z)\}_{4\times1}\right]_0^\ell$, and

$\{F_{zn}(z)\}_{4\times1} = \int_0^\ell \bar{m}_z \{H_\gamma(z)\}_{4\times1} dz + \left[\bar{M}_z(z) \{H_\gamma(z)\}_{4\times1}\right]_0^\ell + \left[\bar{M}_w(z) \{H'_\gamma(z)\}_{4\times1}\right]_0^\ell$.

The above expressions for stiffness, mass and load vector formulated for two-noded beam element with four degrees of freedom per node for each uncoupled response (i.e., lateral, transverse and torsional) are calculated by using the exact shape functions.

9. Examples and Discussion

In this section, several examples are investigated in order to demonstrate the features of the present finite element formulations. In these examples, material is steel with a modulus of elasticity $E = 200GPa$, and shear modulus $G = 70GPa$ and density $\rho = 7{,}850Kg/m^3$, and the dimensions of the doubly symmetric cross-section are; flange width $b = 203mm$, middle surface height, flange thickness $t_f = 13.5mm$, web thickness $t_w = 8mm$. The finite element formulation developed in the present paper is based on the exact shapes functions which exactly satisfy the homogeneous form of the field equations. Due to this treatment, the mesh discretization errors induced in the finite element formulations using polynomial shape functions are eliminated. As a result, it is observed that, the results obtained based on a single finite element in the cantilever beam model (Example 1) and two finite elements for simply-supported beam model (Example 2) exactly matched with those based on the closed-form solutions up to five significant digits. The results obtained are based on three solutions; (1) present solution based on Vlasov beam theory which neglects shear deformation and distortional effects, (2) Abaqus two-noded B31OS beam element model with seven degrees of freedom (i.e., three translations, three rotations and warping deformation) which accounts for shear deformation effects due to bending but neglects the shear

deformation effect due to warping, and distorsional effects, and (3) Abaqus S4R four-noded shell element (with six degrees of freedom per node, i.e., three translation and thee rotations) which accounts for the effects of shear deformation and distortional effects.

9.1 Example 1: Cantilever under Harmonic Transverse Forces – Flexural Response

A 4.0m cantilever beam with a doubly symmetric I-section subjected to transverse harmonic forces; (i) concentrated force $P_y(\ell,t)=8.0e^{i\Omega t}kN$, (ii) concentrated end moment $M_x(\ell,t)=6.0e^{i\Omega t}kNm$ applied at the cantilever free end, and (iii) distributed force $q_y(z,t)=4.0e^{i\Omega t}kN/m$ is considered. The dimensions of the I-section (Fig. 1b) are; flange width $b=203mm$, mid-surface height $H=238.5mm$, flange thickness $t_f=13.5mm$, web thickness $t_f=13.5mm$, and the geometric properties are; $A=7{,}389mm^2$, $I_{xx}=87.10\times10^6mm^4$, $J=373.7\times10^6mm^4$, $C_w=268.0\times10^9mm^6$. This example is aimed at verifying the validity and accuracy of the present finite element formulations. It is required to (1) conduct the quasi-static analysis of the cantilever beam under the given harmonic forces by adopting an exciting frequency $\Omega\approx0.001\omega_1$, and (2) compute a steady state dynamic analysis $\Omega=1.40\omega_1$, where the first natural transverse frequency of the cantilever is $\omega_1=18.83Hz$.

Under the present finite element formulation, the nodal degrees of freedom are obtained using a single finite beam element with eight degrees of freedom per element. In Abaqus shell solution, a total of 3,200 S4R elements ($\approx40{,}570$ dof) are used (six elements per flange, eight elements along web height and one hundred-sixty in the longitudinal direction of the beam), while in Abaqus beam model, a one-hundred B31OS beam elements (≈700 dof) are needed to eliminate the discretization errors.

9.1.1 Quasi-Static Flexural Solution

In order to approach the quasi-static response of the cantilever beam under the given harmonic transverse forces, the exciting frequency Ω is taken significantly lower than the first natural transverse frequency ω_1, i.e., $\Omega\approx0.001\omega_1=0.118rad/\sec$. Table (1) provides the quasi-static response results for the maximum transverse displacement at the free end. The nodal displacement results obtained from the present formulation based on using a single finite element are found identical to the closed-form solution. It is seen that the maximum transverse displacement results obtained from the present finite element solution are in excellent agreement with the Abaqus beam element model but both solutions slightly differ from Abaqus shell element solution by 0.110%-0.188% for Abaqus beam model and by 0.22%-2.88% for the solution developed in the present study. The former differences are due to shear deformation effects due to warping and distortional effects which are not captured by Abaqus B31OS beam element while the later differences are due to shear deformation effects due to shear forces and warping as well as distortional effects which are omitted in the present formulation.

9.1.2 Dynamic Flexural Solution

The steady state transverse response of the cantilever beam under the given harmonic forces with exciting frequency $\Omega=1.328\omega_1=157.1rad/\sec$ is provided in Table (1). The maximum transverse displacement results based on the formulation developed in this study are compared with those based on Abaqus S4R shell and B31OS beam element solutions. It is noted that results obtained from the present finite element formulation based on one beam element (12 dof) provide an excellent agreement with Abaqus beam model based on-hundred (≈700 dof) but both solutions vary from Abaqus shell model based on one hundred sixty S4R shell element (≈40,570 dof) by 3.61% to 5.55% and 2.44% to 3.82% respectively. The first difference is due to shear deformation and distortional effects which are not captured in the present Vlasov solution while the second difference is due to the shear deformation effects due to warping and distorsional effects which are captured by Abaqus Shell model but not in the

Abaqus beam solution. The results provided in Table (1) demonstrate that the shear deformation effects have more significant effects on steady state dynamic analysis than static response analysis.

Table (1): Static and steady state responses results for cantilever under harmonic transverse forces

Type of response	Type of force	Tip transverse displacement in (mm)				
		Abaqus shell solution [1] (40,570DOF)	Abaqus beam solution [2] (700 DOF)	Present finite element [3] (8 DOF)	Difference =[1-2]/1	Difference =[1-3]/1
Static $\Omega \approx 0.001\omega_1$	$P_y(\ell,t)$	10.01	9.866	9.831	1.44%	1.79%
	$M_x(\ell,t)$	2.762	2.759	2.756	0.11%	0.22%
	$q_y(z,t)$	7.568	7.426	7.350	1.88%	2.88%
Steady State $\Omega \approx 1.328\omega_1$	$P_y(\ell,t)$	-12.52	-12.89	-13.01	-2.96%	-3.91%
	$M_x(\ell,t)$	2.957	3.070	3.121	-3.82%	-5.55%
	$q_y(\ell,t)$	-10.26	-10.51	-10.63	-2.44%	-3.61%

9.2 Example 2: Simply-supported I-beam under Torsional Harmonic Loads- Torsional Response

In order to investigate the torsional steady state response, a simply-supported beam is subjected to (1) distributed harmonic twisting moment $m_z(z,t) = 1.20e^{i\Omega t} kNm/m$ and (2) concentrated harmonic twisting moment $M_z(\ell/2,t) = 5.0\, e^{i\Omega t} kNm$ applied at the mid-span of the beam (i.e., $z = \ell/2$). The simply-supported beam has a span $\ell = 5.0m$ and a doubly symmetric cross-section identical to that given in Example 1. In this example, it is required to (i) conduct the steady state torsional response analysis (in which the exciting frequency is varied from nearly zero to 200Hz) and extract the natural torsional frequencies, (ii) investigate the static and steady state torsional dynamic analyses by using two exciting frequencies $\Omega \approx 0.01\omega_{t1}$ and $\Omega = 1.250\omega_{t1}$, respectively. The first natural torsional frequency of the given simply-supported beam is $\omega_{t1} = 24.51Hz$. In order to validate the accuracy and validity of the present formulation, the present finite element solution based on two beam elements with twelve degrees of freedom is compared with (i) Abaqus shell solution using 3,000 S4R element, and (2) Abaqus beam model solution using 100 B31OS beam element are used to eliminate the discretization errors.

9.2.1 Extracting Natural Torsional Frequencies

Under uniformly distributed harmonic twisting moment $m_z(z,t) = 1.20e^{i\Omega t} kNm/m$, the natural torsional frequencies are extracted from the steady state torsional analysis. Table (2) provides the first three natural torsional frequencies of the simply-supported beam. Close agreement is observed between all three solutions. The solution based on the present Vlasov theory predicts the highest natural frequencies values while the Abaqus shell solution predicts the lowest values. In other words, Abaqus shell solution (since it captures the shear deformation and distorsional effects) provides the most flexible model while the present solution provides the stiffest model. The natural frequencies predicted by the present solution differed from 1.59% to 2.68% from those based on Abaqus shell solution.

Table (2): The first three natural torsional frequencies of cantilever I-beam under harmonic torsion

Mode	Abaqus shell solution [1] (37,570dof)	Abaqus beam solution [2] (700dof)	Present finite element [3] (12dof)	Difference =[1-2]/1	Difference =[1-3]/1
1	24.04	24.49	24.51	-1.87%	-1.96%
2	72.43	73.51	73.58	-1.49%	-1.59%
3	149.4	152.1	153.4	-1.81%	-2.68%

9.2.2 Comparison of Torsional Responses

Table (3) provides the static and steady state torsional responses results for the nodal torsional rotation angle at the mid-span of the beam. Results obtained are based on three solutions; (a) the finite element formulation developed in the present study, (b) Abaqus B31OS beam solution, and (c) Abaqus S4R shell element solution. It is noted that, as a general observation, the rotation angle results obtained by the present finite element solution using two-elements having twelve degrees of freedom are closely matched with those determined by the Abaqus beam model using 100 B31OS beam element with 700 dof, but both solutions differ from Abaqus shell solution based on finest mesh (3000 S4R shell element having 37,570 dof). The Abaqus shell element overpredicts the rotation angle by 3.68%-4.23% for static torsional response and by 3.68%-4.37% for steady state torsional response compared with the present study. Again, these differences are due to the inclusion of shear deformation and distorsional effects in the Abaqus shell solution but not in the present solution. As a result, the present formulation provides results in very close agreement with Abaqus shell solution with fewer degrees of freedom.

Table (3): Static and steady state responses for simply-supported I-beam under torsional loads

Type of Analysis	Type of load	Abaqus shell solution [1] (37,570dof)	Abaqus beam solution [2] (1,400dof)	Present finite element [3] (60dof)	Difference =[1-2]/1	Difference =[1-3]/1
Static $\Omega \approx 0.01\omega_{t1}$	$m_z(z,t)$	0.0803	0.0771	0.0769	3.99%	4.23%
	$M_z(\ell/2,t)$	0.1086	0.1050	0.1046	3.31%	3.68%
Steady state $\Omega \approx 1.25\omega_{t1}$	$m_z(z,t)$	0.2476	0.2387	0.2371	3.59%	4.24%
	$M_z(\ell/2,t)$	-0.1854	-0.1774	-0.1773	4.31%	4.37%

9.3 Example 3: Continuous Two-Span beam – Finite element

A two-span beam of a doubly symmetric I-section subjected to two harmonic forces: concentrated transverse force $P_y(6m,t)=15.0e^{i\Omega t}kN$ and distributed transverse force $q_y(z,t)=8.0e^{i\Omega t}kN/m$ is considered as illustrated in Figure (2). The geometric and properties of the doubly symmetric section are given as in Example 1. The first natural frequency for the given beam is $\omega_1=8.877Hz$.

The exciting frequency is assumed to take two values $\Omega \approx 0.001\omega_1$ (quasi-static) and $\Omega = 2.38\bar{\omega}_1$ (steady state response), where the first natural frequency for the continuous beam is $\omega_1=8.877Hz$ in the present problem. It is required to compare the quasi-static and steady state dynamic responses based on the finite element with Abaqus beam element solution.

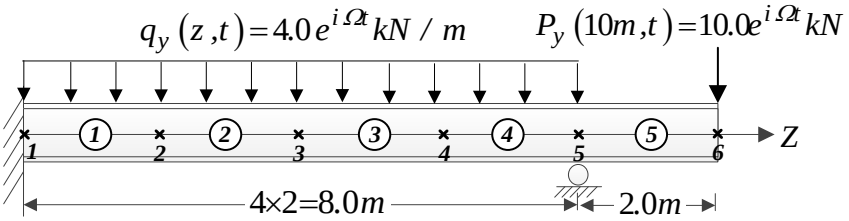

Figure (2): Two-span beam of doubly symmetric I-section under transverse harmonic forces

In order to demonstrate the validity and capability of the present finite element based on Vlasov beam theory, the nodal degrees of freedom results for static transverse response and steady state transverse dynamic response are obtained and compared against the results based on established finite beam element Abaqus. Under the present finite element solution, only five elements with twenty degrees of freedom are used to achieve the convergence while in Abaqus beam analysis, the model is consisted of two-hundred beam B31OS elements with 700 degrees of freedom along the beam axis.

The quasi-static and steady state transverse displacements $\bar{v}(z)$ are plotted against the beam longitudinal coordinate z as illustrated in Figures (1a) and (1b), in which the quasi-static transverse response is approached by using a very low exciting frequency Ω compared to the first natural frequency, i.e., $\Omega\approx0.001\omega_1=0.111rad/\sec$, and the steady state dynamic response is determined for exciting frequency $\Omega=1.417\omega_1\approx157.1rad/\sec$. Compared with Abaqus beam element model (using two-hundred B31OS beam element with 1400 dof) , the finite element formulation developed in present study using five beam elements with twenty degrees of freedom provides an excellent agreement.

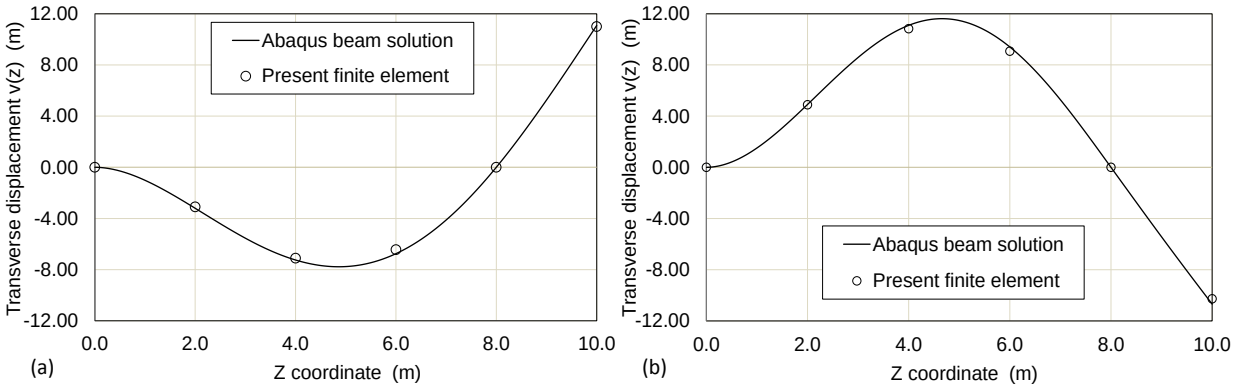

Figure (2): Static and steady state dynamic transverse responses for two-span I-beam

10. Summary and Conclusions

1. A finite element solution is formulated for prismatic thin-walled members of doubly symmetric open cross-sections. The new beam element is based on the exact shape functions were formulated based on the closed-form analytical solutions developed in the companion paper [Hjaji and Mohareb 2013a]. Using the exact shape functions, the variational form of Hamilton's principle was adopted to formulate the exact stiffness, mass matrices and the energy equivalent load vector. The formulation captures the St. Venant and warping deformation effects, translational and rotary inertial effects.
2. The finite elements developed in this study were shown to be free of discretization errors occurred in the conventional finite element.

3. The finite element solution is capable to efficiently capture the static and steady state dynamic responses of beams under various harmonic forces. The solution is also able to capture the eigen-frequencies and eigen-modes of the member.
4. The comparison demonstrated that the new finite element solution provides excellent agreement with Abaqus solutions model while keeping the number of degrees of freedom a minimum.

11. References

Chen, X. and Tamma, K. 1994, Dynamic Response of Elastic Thin-walled Structures Influenced by Coupling Effects, Computers and Structures, 51(1): 91 - 105.

Hashemi S. M., Richard M. J. 2000a, A Dynamic Finite Element Method for Free Vibrations of Bending - Torsion Coupled Beams, Aerospace Sci. Technology, 4: 41 - 55.

Hashemi S. M., and Richard M. J. 2000b, Free vibrational analysis of axially Bending-Torsion Coupled Beams-A dynamic finite element, Computers and structures, 77: 711 - 724.

Hjaji, M. A. and Mohareb, M. 2011, Steady State Harmonic Response of Doubly symmetric Thin-Walled Members-Under Harmonic Loads - Finite Element Formulation, Second International Engineering Mechanics and Materials Specialty Conference, Ottawa, Canada.

Hjaji, M. A. and Mohareb, M. 2013a, Harmonic Response of Doubly symmetric Thin-Walled Members Based on the Vlasov Theory - I. Analytical Solution, Third Specially Conference on Material Engineering and Applied Mechanics, Montreal, Quebec, Canada.

Hu, Y. et al. 1996, A Finite Element Model for Static and Dynamic Analysis of Thin-walled Beams with Asymmetric Cross-Sections, Computers and Structures, 61: 897 - 908.

Kim, N. I. and Kim, M. N. 2005, Exact Dynamic/Static Stiffness Matrices of Non-Symmetric Thin-Walled Beams considering coupled shear deformation effects, Thin-walled Structures, 43: 701-734.

Lee, J. and Kim, S. E. 2002a, Free Vibration of Thin-walled Composite Beams with I-Shaped cross-sections, Composite Structures, 55 (2): 205 - 215.

Lee, J. and Kim, S. E. 2002b, Flexural–torsional coupled vibration of thin-walled composite beams with channel sections, Computers and Structures, 80: 133 -144.

Mei, C. 1970, Coupled vibrations of thin-walled beams of open section using the finite element method, International journal of mechanical science, 12: 883 - 891.

Vlasov, V. 1961, *Thin-walled elastic beams*, 2nd edition, Jerusalem, Israel Prog. for Scientific Translation.

Voros, G. 2008, On Coupled Vibrations of Beams with Lateral Loads, Journal of computational and Applied Mechanics, 9 (2): 1 - 14.

Voros, G. M. 2009, On Coupled bending-torsional vibrations of beams with initial loads, Mechanics Research Communications, 36: 603 - 611.

Vo, T. P. and Lee, J. 2009, Flexural-torsional coupled vibration and buckling of thin-walled open section composite beams using shear-deformable beam theory, International Journal of Mechanics Sciences, 51: 631 - 641.

Vo, T. P. and Lee, J. 2010, Interaction curves for vibration and buckling of thin-walled composite box beams under axial loads and end moments, Applied Mathematical Modelling, 34: 3142 - 3157.

Vo, T. P. et al. 2010, On triply coupled vibrations of axially loaded thin-walled composite beams, Computers and Structures, 88 (3-4): 144 - 153.

Vo, T. P. et al. 2011, Vibration analysis of thin-walled composite beams with I-shaped cross-sections, Composite Structures, 93 (3-4): 812 - 820.